

# Rotationally resolved ultraviolet spectroscopy of indole, indazole, and benzimidazole: Inertial axis reorientation in the $S_1(^1L_b) \leftarrow S_0$ transitions

Giel Berden and W. Leo Meerts

Department of Molecular and Laser Physics, University of Nijmegen, Toernooiveld, 6525 ED Nijmegen, The Netherlands

Erko Jalviste

Institute of Physics, Estonian Academy of Science, Riia 142, EE2400 Tartu, Estonia

(Received 25 July 1995; accepted 24 August 1995)

Rotationally resolved laser induced fluorescence excitation spectra of the  $S_1(^1L_b) \leftarrow S_0$  origin bands of indole, indazole, and benzimidazole have been measured. From these spectra, the rotational constants in both electronic states have been determined. The spectra of all three molecules exhibit "anomalous" rotational line intensities. These intensity perturbations are a result of the reorientation, upon electronic excitation, of the inertial axes of the molecule. Intensity analysis of the rotational lines yielded information about the inertial axis reorientation, and the direction of the transition moment vector for each molecule. © 1995 American Institute of Physics.

## I. INTRODUCTION

The electronic spectra of indole, indazole, and benzimidazole (Fig. 1) are of similar nature. In solution, these molecules have two absorption bands in the near UV, which can be assigned as  $\pi^* \leftarrow \pi$  singlet-singlet transitions.<sup>1</sup> The two excited states are labeled by  $^1L_a$  and  $^1L_b$  following the suggestion of Platt.<sup>2</sup>

Indole has been studied extensively. In solution, both transitions have different properties. First, the  $^1L_b$  absorption band shows vibronic structure with a strong  $0_0^0$  transition, while the  $^1L_a$  absorption band appears to be broad and structureless. Furthermore, the  $^1L_a$  band is very sensitive to the polarity of the solvent, while there is only a little dependence on solvent polarity for the  $^1L_b$  band.<sup>6</sup> In the gas phase, the  $^1L_b$  state is lower in energy than the  $^1L_a$  state.<sup>6</sup> Interaction between indole and polar solvents can bring the  $^1L_a$  state below the  $^1L_b$  state.<sup>7</sup> The origin band of the  $^1L_b$  state is the strongest feature in the vibronically resolved spectrum of jet-cooled indole.<sup>3,4,5</sup> Barstis *et al.*<sup>9</sup> gave an assignment of all spectral features in the excitation spectrum of indole up to  $1000 \text{ cm}^{-1}$  above the  $^1L_b$  origin. They concluded that there is no significant band in the indole spectrum in this interval which can be assigned as belonging to a system other than the  $^1L_b \leftarrow S_0$  transition. Recently, the group of Callis<sup>8</sup> located the  $^1L_a$  vibronic origin in vapor phase indole to be about  $1400 \text{ cm}^{-1}$  above the  $^1L_b$  origin by using polarized fluorescence excitation and dispersed fluorescence techniques on indole in solid Ar at 20 K. Since the  $^1L_a$  state is very sensi-

tive to the environment of the molecule, many studies have been performed on jet-cooled complexes of indole and indole derivatives with polar and nonpolar solvent molecules.<sup>10</sup>

The  $^1L_a$  and  $^1L_b$  states can be distinguished by the direction of the electronic transition moment vector (TM). In solution, analysis of fluorescence excitation and anisotropy spectra can provide the relative direction between the  $^1L_a$  and  $^1L_b$  transition moment vectors, but not the absolute direction in the molecular frame.<sup>13</sup> In the gas phase, the rotationally resolved excitation spectrum can provide the absolute value of the angle between the transition moment vector and the inertial axes. Mani and Lombardi<sup>14</sup> performed a rotational band contour analysis on the room temperature gas phase spectrum of the origin of the  $^1L_b \leftarrow S_0$  transition of indole. They determined the angle  $\theta$  between the  $a$ -axis and the transition moment vector to be  $20^\circ$ . Philips and Levy<sup>15</sup> measured the same transition by using the laser induced fluorescence (LIF) technique in a supersonic molecular jet. They resolved the rotational structure with an experimental resolution of 180 MHz. Analysis of their spectra yielded an angle  $\theta$  of  $45^\circ$ , and the rotational constants in the ground and the electronically excited state. After the LIF study of Philips and Levy, the microwave spectra of indole<sup>16,17</sup> and its N-D isotopomer<sup>17</sup> have been reported.

Indazole and benzimidazole are less thoroughly studied in the gas-phase. For indazole, the vibrationally resolved gas-phase infrared spectrum,<sup>18</sup> and the electronic spectrum<sup>19</sup> have been reported. Precise ground state rotational constants of indazole and its N-D isotopomer have been obtained from microwave spectra reported by Velino *et al.*<sup>20</sup> The same group performed a rotational band contour analysis on the origin band of the  $S_1 \leftarrow S_0$  transition of indazole.<sup>21</sup> All aforementioned measurements were performed in a heated cell. The vibrationally resolved spectrum of the  $S_1 \leftarrow S_0$  transition of benzimidazole has been recorded in a heated cell<sup>22</sup> and in supersonic jet.<sup>23,24</sup> Cané *et al.* reported the microwave spectra of benzimidazole and its N-D isotopomer,<sup>25</sup> and they performed a band contour analysis of the electronic origin.<sup>26</sup>



FIG. 1. The molecular structures of indole, indazole, and benzimidazole.

Indazole might exist in two tautomeric forms; 1H-indazole and 2H-indazole. Catalan *et al.*<sup>27</sup> concluded from spectroscopic and thermodynamic experiments that in the gas-phase, 1H-indazole is the most stable tautomer, both in the ground and excited states. Their conclusion is in agreement with the microwave results, which confirmed the 1H position via isotopic substitution.<sup>20</sup> Recently, we have reported the rotationally resolved fluorescence excitation spectrum of the  $0_0^0$  band of the  $S_1 \leftarrow S_0$  transition of 2H-benzotriazole.<sup>28</sup> The microwave spectra of benzotriazole, recorded in a heated cell<sup>29</sup> and in a jet,<sup>30</sup> have been attributed to the 1H-tautomer. Although 2H-benzotriazole is found to be more stable than 1H-benzotriazole,<sup>31,32</sup> the microwave spectrum of 2H-benzotriazole could not be measured,<sup>30</sup> probably because its permanent dipole moment is too small.<sup>31</sup>

As a result of the low symmetry of indole, indazole, and benzimidazole, different equilibrium molecule-fixed axis systems can exist for ground and electronically excited states. In other words, due to a geometry change in the molecule upon excitation the inertial axes are reoriented. This effect is called axis reorientation, axis switching, axis tilting, or the rotational Duschinsky effect. Axis reorientation has no effect on the frequencies of the rotational lines, but it “perturbs” its intensities. A first fundamental treatment of axis reorientation has been presented in the pioneering work of Hougen and Watson.<sup>33</sup> They explained with this effect the “anomalous” rotational line intensities observed in the spectrum of the  $\tilde{A}^1A_u \leftarrow \tilde{X}^1\Sigma_g^+$  transition of acetylene. Later, axis reorientation in this linear to bent transition of acetylene has been investigated in more detail.<sup>34</sup> Similar effects have been observed in hydrogencyanide.<sup>35</sup> Smalley *et al.*<sup>36</sup> have observed 90° axis reorientation (axis switching) in the excitation spectrum of jet-cooled *s*-tetrazine, and they derived optical selection rules for this special case. This full-angle axis switching effect was also found for other near-oblate symmetric top molecules, like for example pyrimidine.<sup>37</sup> Held *et al.*<sup>38</sup> observed an axis reorientation of 2.4° in the rotationally resolved spectrum of the  $0_0^0$  band of the  $S_1 \leftarrow S_0$  transition of 2-pyridone. Furthermore, they formulated a convenient method to calculate the “anomalous” rotational line intensities. The relation between the axis reorientation effect and the vibrational Dushinsky effect has been elucidated in the theoretical works of Özkan<sup>39</sup> and Chigirev.<sup>40</sup>

In this paper, we present the rotationally resolved fluorescence excitation spectra of the origin bands of the  $S_1(^1L_b) \leftarrow S_0$  transitions of indole, indazole, and benzimidazole. The spectra have been recorded at a Doppler limited resolution of about 15 MHz using a narrow band UV laser system in combination with a molecular beam apparatus. Frequency analysis of the spectra provide accurate values for the rotational constants. All spectra show “anomalous” rotational line intensities, which are an effect of axis reorientation upon electronic excitation. The overall shapes of the spectra have been fit to a model, which includes the axis reorientation effect, to obtain accurate values for the direction of the transition moment vector and the axis reorientation angle. Our results may be useful for testing *ab initio* calculations and for improving semiempirical calculations to

obtain better geometrical and electronic structures of the  $^1L_b$  and  $^1L_a$  excited states of these molecules.

## II. THEORY

Electronic-rotational transitions in a molecule are induced by interactions of the space-fixed radiation field with the rotating electronic transition moment in the (rotating) molecule. Usually, the origin of the molecule-fixed coordinate system is chosen to be at the center of mass of the molecule, and the axes of this frame are chosen to be coincident with the principal axes of inertia of the molecule. The Euler angles  $\theta$ ,  $\phi$ , and  $\chi$  specify the orientation of the rotating molecule-fixed coordinate system with respect to the space-fixed system. The rotational energy levels of the molecules studied in this chapter, can be calculated with an asymmetric rigid rotor Hamiltonian. If the molecule-fixed frame in the ground and excited electronic state are identical, the rotational eigenfunctions of the Hamiltonian in both states can be expressed as a linear combination of the same symmetric top basis functions,  $|JK\rangle$ ,

$$|J''K''K_c''\rangle = \sum_K c''_{J''K} |J''K\rangle, \quad (1)$$

$$|J'K'K_c'\rangle = \sum_K c'_{J'K} |J'K\rangle. \quad (2)$$

The intensity of a single rotational line in the fluorescence excitation spectrum is given by

$$I = I_0 g_n (2J'' + 1) A_{J''K''K_c''J'K'K_c'} \times \exp[-E(J'', K'', K_c'')/kT_{\text{rot}}], \quad (3)$$

where  $I_0$  is a constant,  $g_n$  is the nuclear spin statistical weight, and  $A_{J''K''K_c''J'K'K_c'}$  is the line strength factor. This factor is proportional to the square of the electronic transition moment matrix element

$$A_{J''K''K_c''J'K'K_c'} \propto |\langle J''K''K_c'' | \mu_F | J'K'K_c' \rangle|^2, \quad (4)$$

where  $\mu_F$  is the electronic transition moment vector component along the space-fixed axis  $F = X, Y, Z$ , which can be expressed in components along the molecule-fixed axes  $\mu_g$ ,

$$\mu_F = \sum_g \cos(Fg) \mu_g \quad g = a, b, c, \quad (5)$$

where  $\cos(Fg)$  are the direction cosines. Since the rotational eigenfunctions of the ground and excited electronic states are expressed in the same basis set, the line strength factor [Eq. (4)] can be evaluated.

The ground and excited state rotational eigenfunctions and the direction cosines operators can be classified according to their symmetry under the Four-group (dihedral group  $D_2$ ).<sup>41</sup> It can then be shown that the sum in Eq. (5) contributes to the line strength factor with only one term, and each transition can be labeled uniquely as *a*, *b*, or *c* type.<sup>41</sup>

The geometry of a molecule usually changes upon electronic excitation. Above, it was assumed that the molecule-fixed frames in both electronic states are identical. This requires that the geometry change in the molecule should be

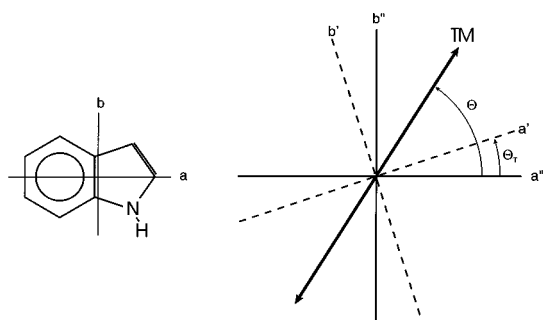


FIG. 2. Schematic of the indole geometry and its principal axis system (left). Definition of the axis reorientation angle  $\theta_T$  and the direction of the transition moment (TM) vector  $\theta$ . The angles measured in the counterclockwise sense are taken to be positive.  $a''$  and  $b''$  are the principal axes in the ground state,  $a'$  and  $b'$  are the principal axes in the excited state. The  $c$  axes are perpendicular to the molecular plane.

such that the principal axes do not change their orientation. If a molecule has “high” symmetry (e.g., naphthalene or 2H-benzotriazole) this will indeed be the case (see Refs. 33, 39, and 40 for a discussion of the relation between the symmetry of a molecule and the axis reorientation effect). For molecules with “low” symmetry, electronic excitation can (but does not have to) change the geometry in a way that the principal axes are reoriented with respect to the space fixed frame. Therefore, two rotating molecule-fixed coordinate systems are required to describe the rotational motion of the molecule if electronic excitation takes place. The relative orientation in space of both molecule-fixed systems remains constant and is solely defined by the geometry change.

The rotational energy levels in both electronic states can still be calculated using the asymmetric rotor Hamiltonian for each state in its principal axis system. However, the resulting rotational eigenfunctions for both states are now expressed on different symmetric top basis sets,  $|JK\rangle''$  and  $|JK\rangle'$  (both sets are defined in their own molecule-fixed coordinate system). In order to calculate the line strength factor [Eq. (4)] both eigenfunctions should be expressed in the same basis set.

In their original description of the axis reorientation effect, Hougen and Watson,<sup>33</sup> defined a transformation matrix  $\mathcal{D}_{K'K}^{(J')}( \theta_T, \phi_T, \chi_T )$  to transform the rotational basis set of the excited state to that of the ground state,  $|JK\rangle''$ ,

$$|J'K'_aK'_c\rangle = \sum_K c_{J'K} \sum_{K'} \mathcal{D}_{K'K}^{(J')}( \theta_T, \phi_T, \chi_T ) |JK\rangle'' \quad (6)$$

Now, both the ground and the electronic excited state rotational eigenfunctions are expressed in the same basis, and thus, the line strength factor can be evaluated.

Held *et al.*<sup>38</sup> have observed anomalous intensities in the fully resolved  $S_1 \leftarrow S_0$  electronic spectrum of 2-pyridone. These effects have been attributed to axis reorientation in the plane of the molecule. They used a more convenient method to calculate the line strengths. Instead of transforming the excited state eigenfunctions into the coordinate system of the ground state, they first expressed the excited state Hamiltonian in the principal axis system of the ground state. Di-

agonalizing the transformed excited state Hamiltonian gives the same rotational energy eigenvalues as the “unswitched” Hamiltonian, but the eigenfunctions are now defined on the same basis set as the ground state eigenfunctions.

In indole, indazole, and benzimidazole, the reorientations of the principal axes are also in the plane of the molecule. This means that in both electronic states the  $c$ -axes coincide. The relative orientation between both sets of principal axes is then described with one parameter; the angle  $\theta_T$  that rotates the  $a$ -axis of the ground state into the  $a$ -axis of the excited state (Fig. 2). The components of the rotational angular momentum operator in the excited state in the principal axis system of that state  $J'_g$  can be expressed in the components in the principal axis system of the ground state  $J_g$  by a simple  $3 \times 3$  rotation matrix,

$$\begin{pmatrix} J'_a \\ J'_b \\ J'_c \end{pmatrix} = \begin{pmatrix} \cos \theta_T & \sin \theta_T & 0 \\ -\sin \theta_T & \cos \theta_T & 0 \\ 0 & 0 & 1 \end{pmatrix} \begin{pmatrix} J_a \\ J_b \\ J_c \end{pmatrix} \quad (7)$$

The Hamiltonian of the excited state expressed in the molecule-fixed frame of the ground state is then given by

$$\begin{aligned} H' = & (A' \cos^2 \theta_T + B' \sin^2 \theta_T) J_a^2 \\ & + (A' \sin^2 \theta_T + B' \cos^2 \theta_T) J_b^2 + C' J_c^2 \\ & + (A' - B') \sin \theta_T \cos \theta_T (J_a J_b + J_b J_a) \end{aligned} \quad (8)$$

The term containing the cross products of the angular momentum components generates new off-diagonal matrix elements in the excited state Hamiltonian.

The excited state Hamiltonian has no longer the Four-group symmetry of the ground state due to the angular momentum cross terms. This means that the sum in Eq. (5) contributes with more than one term to the line strength factor. Therefore the rotational lines cannot be labeled uniquely as  $a$ ,  $b$ , or  $c$  type. However, we still will use this labeling, which gives then the dominant character of a particular line. For indole, indazole, and benzimidazole, the transition moment vector is in the plane of the molecule, therefore the line strength factor becomes

$$\begin{aligned} A_{J''K''_aK''_c, J'K'_aK'_c} \propto & |\langle J''K''_aK''_c | \cos(Fa) \mu_a | J'K'_aK'_c \rangle|^2 \\ & + |\langle J''K''_aK''_c | \cos(Fb) \mu_b | J'K'_aK'_c \rangle|^2 \\ & + 2 \langle J''K''_aK''_c | \cos(Fa) \mu_a | J'K'_aK'_c \rangle \\ & \times \langle J''K''_aK''_c | \cos(Fb) \mu_b | J'K'_aK'_c \rangle \end{aligned} \quad (9)$$

Without axis reorientation, only the first or second term would be nonzero (giving, respectively, an  $a$  or  $b$  type transition). For axis reorientation in the  $ab$ -plane, the symmetry is reduced from  $D_2$  to  $C_2(c)$ , the cyclic group containing a rotation of  $\pi$  around the  $c$ -axis. The lowered symmetry of the Hamiltonian<sup>42</sup> leads to less stringent rotational selection rules. The selection rules for the transition moment components along the  $a$  and  $b$ -axis are now identical,  $K''_c \rightarrow K'_c = e \leftrightarrow o$ . The  $K_a$  parity is no longer distinguished.<sup>43</sup> Therefore, both components contribute to the same rotational transition.

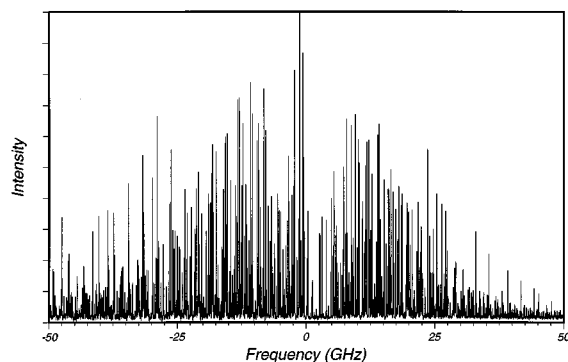


FIG. 3. High resolution LIF spectrum of the origin of the  $S_1 \leftarrow S_0$  transition of indole. The absolute frequency of the origin (0.0 on the scale of the figure) is at  $35\,231.420 \pm 0.006 \text{ cm}^{-1}$ .

What is the effect of axis reorientation on the intensities of for example indazole? In this molecule, the electronic transition moment vector makes an angle of  $62^\circ$  with the  $a$ -axis, and the reorientation angle is only  $1^\circ$ . Without axis reorientation, the spectrum exhibits  $ab$ -type hybrid band character. Turning the axis reorientation on, certain  $a$ -type lines lose (or gain) intensity and certain  $b$ -type lines gain (or lose) intensity in a way that the total line strength and intensity from a given initial state is conserved. For a more extensive discussion about the intensity effects, we refer to Hougén and Watson<sup>33</sup> and Held, Champagne, and Pratt.<sup>38</sup>

### III. EXPERIMENT

Rotationally resolved fluorescence excitation spectra of indole, indazole, and benzimidazole were obtained using a narrow bandwidth UV laser system and a molecular beam apparatus. Indole (Janssen Chimica, 99%), indazole (Fluka, 99%), and benzimidazole (Janssen Chimica, 98%) were heated to  $\sim 50^\circ\text{C}$ ,  $100^\circ\text{C}$ , and  $175^\circ\text{C}$ , respectively, seeded in 0.5 bar argon, and expanded through a nozzle with a diameter of 0.15 mm. The nozzle was kept at a slightly higher temperature to prevent condensation of the sample in the orifice. The molecular beam was skimmed twice in a differential pumping system and was crossed perpendicularly with a UV laser beam at about 30 cm from the nozzle.

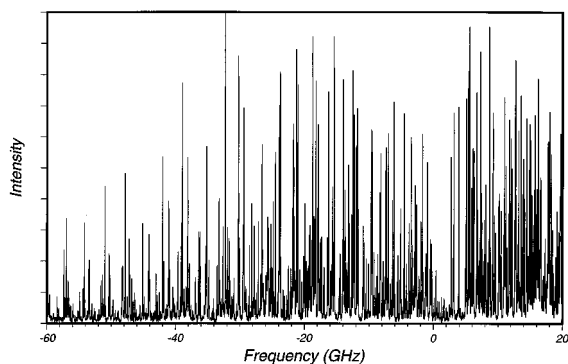


FIG. 4. High resolution LIF spectrum of the origin of the  $S_1 \leftarrow S_0$  transition of indazole. The absolute frequency of the origin (0.0 on the scale of the figure) is at  $34\,471.691 \pm 0.006 \text{ cm}^{-1}$ .

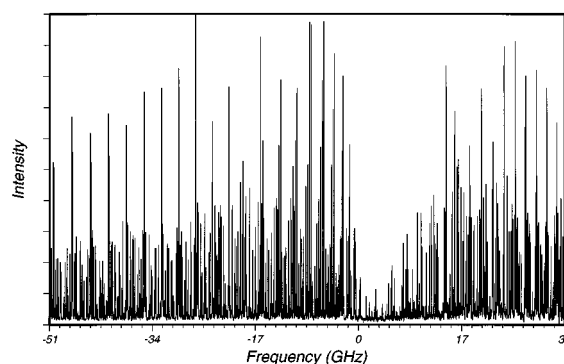


FIG. 5. High resolution LIF spectrum of the origin of the  $S_1 \leftarrow S_0$  transition of benzimidazole. The absolute frequency of the origin (0.0 on the scale of the figure) is at  $36\,021.336 \pm 0.006 \text{ cm}^{-1}$ .

UV radiation with a bandwidth of 3 MHz was generated by intracavity frequency doubling in a single frequency ring dye laser operating on Rh110. By using a 2 mm thick Brewster cut BBO crystal, 0.1–0.3 mW of tunable radiation was obtained. For relative frequency calibration a temperature stabilized Fabry–Perot interferometer was used with a free spectral range of 75 MHz. For absolute frequency calibration, the iodine absorption spectrum<sup>44</sup> was recorded simultaneously. The total undispersed fluorescence was imaged on a photomultiplier connected to a photon counting system interfaced with a computer.

### IV. RESULTS AND INTERPRETATION

#### A. Frequency analysis

The high resolution fluorescence excitation spectra of the origin bands of the  $S_1 \leftarrow S_0$  transitions of indole, indazole, and benzimidazole are shown in Figs. 3, 4, and 5, respectively. Each observed spectrum is an  $ab$ -hybrid band. No  $c$ -type character was found. Each spectrum consists of about 2000 lines, and spans approximately  $5 \text{ cm}^{-1}$ . The absolute frequencies of the origins are given in Table I.

As a starting point for the rotational assignment, each spectrum was simulated using a rigid asymmetric rotor Hamiltonian and rotational constants reported in other studies. The rotational ground state constants were taken from microwave experiments (indole,<sup>17</sup> indazole,<sup>20</sup> benzimidazole<sup>25</sup>). The excited state constants and the hybrid characters were taken from rotational band contour studies in a supersonic jet (indole<sup>15</sup>), or in the vapor phase (indazole,<sup>21</sup> benzimidazole<sup>26</sup>). Unique assignments could be made by comparing the simulations with the experimental spectra. All lines could be fitted within the experimental error. The obtained ground state constants overlap within their errors with the microwave constants. Since the latter constants are two orders of magnitude more accurate than our constants, the UV data have been fitted again with the ground state constants kept fixed to the microwave values. This method gives more accurate excited state constants. The results are shown in Table I; listed are the rotational constants in the  $S_0$  state and their differences with those in the  $S_1$  state. Furthermore, the asymmetry parameters and the inertial defects in both

TABLE I. Molecular constants of indole, indazole, and benzimidazole in the ground state (double prime) and the excited state (single prime).  $A$ ,  $B$ , and  $C$  are the rotational constants.  $\Delta I$  is the inertial defect ( $\Delta I = I_c - I_b - I_a$ ).  $\kappa$  is the asymmetry parameter.  $\nu_0$  is the absolute frequency of the origin.  $\theta$  is the angle between the inertial  $a$ -axis and the electronic transition moment vector.  $\theta_T$  is the axis reorientation angle. The signs of  $\theta$  and  $\theta_T$  signs are coupled; the upper signs or the lower signs.

	Molecular constants			
	Indole <sup>a</sup>	Indazole <sup>b</sup>	Benzimidazole <sup>c</sup>	
$A''$	3 877.828(6)	3 977.927(6)	3 929.720(7)	MHz
$B''$	1 636.047(1)	1 633.272(1)	1 679.259(3)	MHz
$C''$	1 150.899 7(8)	1 158.141(1)	1 176.747(1)	MHz
$A' - A''$	-134.751(6)	-102.220(11)	-155.687(7)	MHz
$B' - B''$	-17.918(14)	-29.235(18)	-15.294(5)	MHz
$C' - C''$	-20.73(1)	-23.24(6)	-21.437(8)	MHz
$\Delta I''$	-0.111 3(7)	-0.102 3(8)	-0.086 6(11)	amu $\text{\AA}^2$
$\Delta I'$	0.168(8)	-0.158(26)	-0.188 9(6)	amu $\text{\AA}^2$
$\kappa''$	-0.644 180 3(16)	-0.663 002 1(15)	-0.634 931 3(32)	
$\kappa'$	-0.626 500(15)	-0.657 667(23)	-0.611 524(10)	
$\nu_0$	35 231.420(6)	34 471.691(6)	36 021.336(6)	cm <sup>-1</sup>
$\theta$	$\pm 38.3(2)^\circ$	$\pm 62.2(7)^\circ$	$-22.0(8)^\circ$	
$\theta_T$	$\pm 0.50(9)^\circ$	$\pm 1.03(11)^\circ$	$\pm 0.72(10)^\circ$	

<sup>a</sup>Ground state constants obtained from microwave experiments (Ref. 17).

<sup>b</sup>Ground state constants obtained from microwave experiments (Ref. 20).

<sup>c</sup>Ground state constants obtained from microwave experiments (Ref. 25).

states are given. Clearly, all three molecules are planar asymmetric tops in both states (inertial defects are small and  $\kappa \approx -0.6$ ). The excited state constants obtained from Table I are in agreement with the reported constants obtained from rotational band contour analysis,<sup>15,21,26</sup> but are more accurate since they have been obtained from well resolved rotational spectra.

## B. Intensity analysis

The direction of the electronic transition moment vector is determined by the hybrid character of the spectrum. For all three molecules, this vector is in the plane of the molecule since no  $c$ -type lines have been observed. If  $\theta$  is the angle between the electronic transition moment vector and the  $a$ -axis,  $I^b$  is the experimental intensity of a particular  $b$ -type line, and  $I^a$  is the experimental intensity of an  $a$ -type line originating from the same rotational ground state level, the angle  $\theta$  can be calculated from

$$\tan^2 \theta = \frac{I^b A_a}{I^a A_b}, \quad (10)$$

where  $A_a$  and  $A_b$  are the line strength factors.

Without axis reorientation,  $\theta$  can be determined by a careful examination of the intensities of rotational lines. To eliminate rotational temperature effects, at least two fully resolved lines have to be found which originate from the same ground state level, but have different character. Since the effect of axis reorientation is a "transfer of intensities" between  $a$ - and  $b$ -type lines, at least three fully resolved lines are needed to determine both  $\theta$  and the reorientation angle  $\theta_T$ . If the molecule is "small" and the rotational lines are narrow, it is possible to locate such a set of lines, and both angles can be determined. However, for indole, indazole, and benzimidazole such a set of lines is difficult to find or even does not exist. This is due to the small rotational

constants of these molecules, which result in many overlapping rotational lines. However, the information needed is still present in every rotational transition, i.e., in the entire spectrum. Therefore, we decided to perform a least-squares fit of the intensity contour of the total spectrum. This contour is determined not only by  $\theta$  and  $\theta_T$ , but also by the rotational temperature and the linewidth of each transition.

The rotational contours were calculated using the rotational constants from Table I, and variable parameters for the rotational temperature, the hybrid character ( $\theta$ ), the reorientation angle ( $\theta_T$ ), and the linewidth. These parameters were varied in a least-squares fitting program. The  $\chi^2$  value to be minimized was calculated as the sum of the squared differences between the intensities of the simulated and experimental spectra. The maximum number of points on the frequency scale was 20 000. If the spectrum contained more points, the number of points was reduced after first smoothing the spectrum. Besides the fitted parameters, the residual spectrum (the difference between the experimental and calculated spectra) was obtained.

The full width at half maximum (FWHM) of single rotational lines can be directly obtained from the spectra. The results are 22(1) MHz for indole, 35(2) MHz for indazole, and 21(1) MHz for benzimidazole. These values are larger than the instrumental linewidth, which amounts about 15 MHz (mainly a result of residual Doppler broadening). This instrumental line profile can be best approximated with a Gaussian profile.<sup>45</sup> Since it is expected that the rotational lines are homogeneously broadened due to a finite lifetime in the excited state, we used a Voigt profile to describe the line shape of every rotational transition. The parameters to be varied were the Lorentzian linewidth  $\Delta\nu_L$ , and the Gaussian linewidth  $\Delta\nu_G$ .

The results of the contour fitting of several spectra of

TABLE II. Results of the intensity analysis of indole, indazole, and benzimidazole. The first column, marked with #, gives the number of the spectrum which has been analyzed. The second column (Model) gives the number of the models which have been used to analyze the spectra. The 4 models with their parameters are described Table III. See the text for further details.

#	Model	$\theta$ deg	$\theta_T$ deg	$T_1, T_J$ K	$T_2, T_K$ K	$W$	$\Delta\nu_L$ MHz	$\Delta\nu_G$ MHz	$\chi^2$ a.u.
Indole									
1	1	38.62	0.58	2.62	...	...	8.1	19.0	440
1	2	38.46	0.58	1.60	5.51	0.192	10.1	17.6	182
1	3	38.48	0.53	2.60	2.63	...	8.1	19.0	440
1	4	38.34	...	1.61	5.62	0.184	10.0	17.7	213
2	1	38.56	0.37	2.49	...	...	9.3	18.2	188
2	2	38.30	0.43	1.49	4.83	0.243	10.8	17.0	104
2	3	38.66	0.39	2.45	2.70	...	9.5	18.1	185
2	4	37.88	...	1.49	4.80	0.245	10.8	17.0	112
3	1	38.34	0.54	2.61	...	...	9.2	18.2	308
3	2	38.22	0.58	1.84	6.39	0.134	10.6	17.1	202
3	3	38.42	0.58	2.56	2.78	...	9.3	18.1	305
3	4	37.58	...	1.85	6.54	0.128	10.7	17.0	224
4	1	38.40	0.44	2.47	...	...	9.3	17.4	632
4	2	38.18	0.42	1.72	5.63	0.159	10.4	16.6	340
4	3	38.46	0.46	2.43	2.64	...	9.4	17.3	606
4	4	37.68	...	1.68	5.40	0.179	10.4	16.6	371
Indazole									
1	1	62.57	1.06	3.90	...	...	24.3	20.0	101
1	2	62.39	1.14	2.76	8.55	0.165	25.5	18.7	64
1	3	62.57	1.07	3.90	3.91	...	24.3	20.0	101
1	4	63.31	...	2.62	7.40	0.235	24.7	19.5	83
2	1	63.06	0.92	3.89	...	...	25.5	18.6	111
2	2	62.79	1.02	2.59	8.03	0.199	26.8	17.2	54
2	3	63.07	0.91	3.86	3.88	...	25.5	18.6	111
2	4	63.57	...	2.65	8.07	0.191	26.3	17.7	72
3	1	62.15	0.99	3.32	...	...	26.7	19.0	122
3	2	61.98	1.03	1.98	6.28	0.376	26.7	18.9	97
3	3	62.52	1.04	3.18	3.79	...	26.8	18.9	120
3	4	61.39	...	1.77	5.45	0.571	27.1	18.5	119
4	1	62.46	1.09	3.42	...	...	25.2	10.9	145
4	2	61.54	0.94	2.42	8.92	0.170	26.9	16.4	98
4	3	62.20	1.01	3.31	4.31	...	25.8	17.4	139
4	4	58.24	...	2.26	8.59	0.211	27.5	15.7	121
Benzimidazole									
1	1	19.57	1.07	12.7	...	...	11.6	15.5	184
1	2	21.24	0.74	6.18	20.4	0.54	11.3	15.7	137
1	3	22.69	0.68	11.1	14.7	...	11.7	15.4	170
1	4	22.48	...	5.57	20.0	0.51	11.4	15.7	145
2	1	22.34	0.57	10.1	...	...	11.0	15.5	155
2	2	22.23	0.65	4.13	15.6	0.80	11.3	15.3	130
2	3	23.68	0.81	8.19	12.1	...	11.7	15.1	146
2	4	21.78	...	5.10	21.8	0.51	11.3	15.4	134
3	1	22.17	1.08	9.91	...	...	11.7	15.6	53
3	2	22.60	0.78	4.84	19.9	0.42	11.8	15.4	39
3	3	23.34	0.71	9.06	13.4	...	11.3	15.8	49
3	4	21.22	...	5.05	21.6	0.38	11.6	15.5	41

indole, indazole, and benzimidazole are given in Table II. The meaning of the different simulation models is presented in Table III. Model 1 assumes an exponential population distribution (Boltzmann distribution). There are two possible sets of  $(\theta, \theta_T)$  values which fit each spectrum. For example, for the first spectrum of indazole,  $\theta = +62.57^\circ$  and  $\theta_T = +1.06^\circ$ , as well as,  $\theta = -62.57^\circ$  and  $\theta_T = -1.06^\circ$ , describe the spectra equally well. The residual spectrum, however,

showed a rather poor agreement with the experimental data; the lines originating from the lowest and highest rotational levels in the  $S_0$  were underestimated. This observation is not surprising, since it is known that the rotational state distribution in the molecular beam is non-Boltzmann (nonequilibrium).<sup>46</sup>

Wu and Levy<sup>47</sup> used a three-parameter two-temperature distribution which is given by

TABLE III. The different models used for the intensity analysis of the spectra of indole, indazole, and benzimidazole (Table II). Most of the parameters are defined in the text.  $\Delta\nu_L$  is the Lorentzian line width (FWHM),  $\Delta\nu_G$  is the Gaussian linewidth (FWHM), BG is the background in the spectrum, and ISF is an intensity scaling factor. See text for further details.

Model	Short description	Parameters								
1	Boltzmann distribution	$\theta$	$\theta_T$	$T_1$			$\Delta\nu_L$	$\Delta\nu_G$	BG	ISF
2	Two-temperature distribution [Eq. (11)]	$\theta$	$\theta_T$	$T_1$	$T_2$	$W$	$\Delta\nu_L$	$\Delta\nu_G$	BG	ISF
3	Two-temperature distribution [Eq. (12)]	$\theta$	$\theta_T$	$T_J$	$T_K$		$\Delta\nu_L$	$\Delta\nu_G$	BG	ISF
4	Model 2, no axis reorientation	$\theta$		$T_1$	$T_2$	$W$	$\Delta\nu_L$	$\Delta\nu_G$	BG	ISF

$$n_{J,K_a,K_c}(T_1,T_2,W) = e^{-E_{JK_aK_c}/kT_1} + We^{-E_{JK_aK_c}/kT_2}, \quad (11)$$

where  $n_{J,K_a,K_c}$  is the population in level  $(J,K_a,K_c)$  of the electronic and vibrational ground state, which has an energy  $E_{J,K_a,K_c}$ .  $T_1$  is the lower temperature and  $T_2$  the higher one.  $W$  is a weighting factor. This distribution can be considered to describe a mixture of two ensembles, one with temperature  $T_1$  and the other with temperature  $T_2$ . Introducing this distribution greatly improves the contour fitting as shown in Table II (model 2). For all spectra the  $\chi^2$  value is lowered. Also the background intensity is decreased (not shown in table), indicating that the fit describes the experimental spectrum more entirely. It should be noted that the variation of the molecular beam conditions (backing pressure, temperature of sample) results in different rotational temperatures for different spectra of the same molecule.

An alternative non-Boltzmann distribution is given by

$$n_{J,K_a,K_c}(T_J,T_K) = e^{-E_{J0J}/kT_J} e^{-(E_{JK_aK_c} - E_{J0J})/kT_K}, \quad (12)$$

where  $T_J$  is the rotational temperature of the  $J$  manifold, and  $T_K$  that of the  $K$  manifold. In this distribution, the rotational population is no longer a one-valued function of the total energy [like the distribution in Eq. (11)]. Rotational population analysis of jet-cooled glyoxal performed by Pebay Peyroula and Jost<sup>48</sup> clearly revealed that rotational cooling is more efficient for  $J$  states with the same  $K$  value, than for  $J$  states with different  $K$  values, i.e.,  $T_J < T_K$ . This two temperature distribution was also used by Price *et al.*<sup>49</sup> for simulation of the excitation spectrum of jet-cooled acetaldehyde. The results for indole, indazole, and benzimidazole are given in Table II (model 3).

The first two-temperature distribution [Eq. (11)] describes the experimental spectrum better than the second one, since the  $\chi^2$  values for model 2 are always better than those for model 3 (Table II). The values of the temperatures  $T_J$  and  $T_K$  are very close to each other for all three molecules. This indicates that the distribution given by Eq. (12) is close to a Boltzmann distribution. Therefore, it is not surprising that the values of  $\theta$ ,  $\theta_T$ , the linewidths, and  $\chi^2$ , of model 3 are almost identical to those of model 1. The question arises why the distribution of Eq. (12) gives no improvement in describing the spectra compared with the simple Boltzmann distribution, while it clearly describes the rotational distributions in glyoxal and acetaldehyde. This can be explained by the differences in rotational population formation during the cooling process due to the qualitatively different rotational energy level structure of these molecules. Both molecules are

near prolate symmetric tops which have large  $K$ -spacing compared with  $J$ -spacing, leading to  $T_J < T_K$ , because the population transfer between neighbouring  $K$ -levels is more restricted. Indole, indazole, and benzimidazole are very asymmetric molecules, leading to a different ground state energy level structure for which the distribution of Eq. (12) does not hold. Theoretically, the results for  $\theta$  and  $\theta_T$  should not depend much on the choice of the temperature distribution model, since the hybrid character and axis reorientation are effective on all rotational levels. From Table II, it is seen that the results for a single spectrum (model 1, 2, and 3) are in reasonable agreement.

To check whether the results for the hybrid character and the axis reorientation angle depend on the chosen line profile, we have fit the spectra using a Gaussian line profile, and a Lorentzian profile. Although the use of these alternative profiles describe the spectra worse than the Voigt profile (higher  $\chi^2$  and worse residual spectra), the values of  $\theta$  and  $\theta_T$  are within their experimental error equal to those obtained when using a Voigt profile. More generally, although the intensity shape of a spectrum is determined by the direction of the transition moment vector, the axis reorientation effect, the rotational population distribution, and the line profile of the rotational lines, it is possible to extract accurate information about the transition moment and the axis reorientation, without knowing the actual state distribution and line profile. The final values of  $\theta$  and  $\theta_T$  presented in Table I were obtained by averaging the results for model 2.

Since our intensity analysis of a particular spectrum is based on the results of the frequency analysis of the same spectrum, it is important to consider how small variations of the fixed rotational constants influence the results of the contour fitting (in particular  $\theta$  and  $\theta_T$ ). Therefore, we have fit the intensities of the second spectrum of indole (Table II) for different sets of rotational constants. These rotational constants were varied within their errors. In the worst case, the relative changes in  $\theta$  and  $\theta_T$  were only 0.1% and 5%, respectively.

In Fig. 6 portions of the  $P$  and  $R$  branches of indazole are shown to illustrate the effects of axis reorientation on the intensities of individual rotational lines. A simulation of both portions obtained by using the values of  $\theta$  and  $\theta_T$  of Table I, is shown in the second row of Fig. 6. The transitions originating from the ground states (8,0,8) and (8,1,8) are labeled. Temperature effects on the intensities are for these lines unimportant since both lines are nearly isoenergetic. The third row of Fig. 6 shows a simulation obtained by fitting the

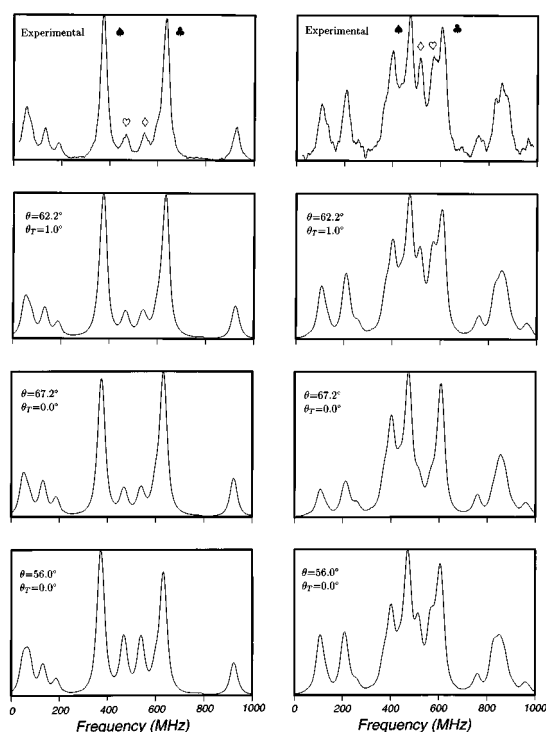


FIG. 6. Portions of the  $P$  branch (left column) and  $R$  branch (right column) of indazole. Top row, experimental parts; horizontal scales are relative. Four transitions in each branch are labeled.  $P$  branch, ♠=(7,0,7)←(8,1,8); ♥=(7,0,7)←(8,0,8); ♦=(7,1,7)←(8,1,8); ♣=(7,1,7)←(8,0,8).  $R$  branch, ♠=(9,0,9)←(8,1,8); ♦=(9,1,9)←(8,1,8); ♥=(9,0,9)←(8,0,8); ♣=(9,1,9)←(8,0,8). Second row, simulations using the constants from Table I. Third row, results of the intensity fit of the  $P$  branch without axis reorientation ( $\theta_r=0$ ). Last row, results of the intensity fit of the  $R$  branch without axis reorientation.

intensities of the  $P$  branch lines, while neglecting axis reorientation ( $\theta_r=0$ ). A hybrid angle of  $67.2^\circ$  describes the  $P$  branch lines good, but the agreement with the experimental lines in the  $R$  branch is very poor (now, the lines labeled with ♠ and ♣ are pure  $b$ -type lines, while the lines labeled with ♥ and ♦ are pure  $a$ -type lines). In a similar way, the  $R$  branch intensities can be fit. Now, an angle of  $56.0^\circ$  gives good agreement in the  $R$  branch, but very poor agreement in the  $P$  branch. It should be noted that the quadruplets in Fig. 6 are not fully resolved.

Figure 6 shows the effect of neglecting axis reorientation when fitting a small part of a spectrum. We have also fit the entire spectra of indole, indazole, and benzimidazole using the temperature model of Eq. (11) and neglecting axis reorientation. The results are shown in Table II (model 4). Comparison of the  $\theta$  values show that  $\theta$  is only slightly altered by introducing axis reorientation. Since axis reorientation alters the intensities of rotational lines in a way that the total line strength and intensity from a given initial state is conserved, it is expected that both models should give exactly the same value for  $\theta$ . However, only about 80% of a spectrum has been fit at once. Therefore, intensity can “transfer” in or out of that part, causing small deviations in the value for  $\theta$  when comparing the fitting results with and without axis reorientation.

The Gaussian contribution to the linewidth of benzimidazole (model 2) is equal to the expected instrumental linewidth ( $\sim 15.5$  MHz). The lifetime, obtained from the Lorentzian contribution, is then estimated to be  $14 \pm 4$  ns. The Gaussian contribution for indole and indazole (respectively, 17.1 and 17.8 MHz), are larger than expected. The lifetime of indole is known to be  $17.6 \pm 0.1$  ns.<sup>10</sup> This leads to a Lorentzian contribution of 9.0 MHz, which is slightly smaller than the experimental value of 10.5 MHz. Although speculative, the observed broadening of the rotational lines of indole and indazole may be caused by unresolved hyperfine splitting. Hyperfine splitting has been observed in the microwave spectra of indole<sup>16</sup> and pyrazole.<sup>50</sup>

## V. DISCUSSION

From the well resolved rotational spectra, accurate values for the directions of the transition moment vectors of indole, indazole, and benzimidazole have been obtained. For indole, the results of the present study can be compared with results from earlier studies, which did not take axis reorientation into account. Philips and Levy<sup>15</sup> measured the fluorescence excitation spectrum of indole in a supersonic jet at a resolution of 180 MHz. Their best fit to the spectrum was produced with equal mixtures of  $a$ - and  $b$ -type spectra, resulting in a  $|\theta|$  of  $45^\circ \pm 5^\circ$ . This value is slightly higher than our value,  $38.3^\circ \pm 0.2^\circ$ . Mani and Lombardi<sup>14</sup> analyzed the absorption spectrum at room temperature at a resolution of  $0.05 \text{ cm}^{-1}$ . Although they obtained a best fit with a 70%  $a$ -type and 30%  $b$ -type transition ( $|\theta|=33^\circ$ ), they reported a hybrid character of 80%  $a$ -type and 20%  $b$ -type ( $|\theta|=27^\circ$ ), since they thought that the  $b$ -type character was overestimated as a result of neglecting  $J>80$  (limited computer memory). However, Philips and Levy have shown that this was not the case, and concluded that a value of  $33^\circ$  is the better one.<sup>15</sup> Comparing the  $\theta$  values obtained from the fits with models 2, and 4 (Table II), shows that approximately the same values are found. Therefore, intensity analysis of the *total* spectrum, with or without taking axis reorientation into account, should give the same values for  $\theta$ . However, both Philips and Levy,<sup>15</sup> and Mani and Lombardi<sup>14</sup> used only part of the spectrum to determine the hybrid character. This explains the deviations in the values for the direction of the transition moment vector of indole.

From Eq. (10), it is seen that only the absolute value of  $\theta$  can be determined, and not its sign. Therefore, two directions for the transition moment vector are possible,  $+38.3^\circ$  and  $-38.3^\circ$ . In tryptamine, the  $a$ -axis is rotated away from the nitrogen atom in the indole chromophore. Philips and Levy<sup>51</sup> analyzed the rotational band contour of jet-cooled tryptamine, and concluded that the transition moment vector is located at  $59^\circ$  with respect to the indole  $a$ -axis. Since the substitution of the ethylamine group causes only a small perturbation in the direction of the transition moment, they concluded that the plus sign should be taken for the angle  $\theta$  of indole.<sup>51</sup> Therefore, we conclude that  $\theta = +38.3^\circ$ . The plus sign for indole is consistent with theoretical results of Callis.<sup>52,53</sup> The values of  $\theta$ , calculated by different methods, are in the range of  $+32^\circ$  to  $+76^\circ$ . Because the axis reorien-

tation angle  $\theta_T$  has the same sign as  $\theta$  (see Table I), it follows immediately that  $\theta_T = +0.50^\circ$ .

For indazole, the results of the earlier study from Cané *et al.*<sup>21</sup> are in disagreement with the results of present study. From the results of a computer simulation of the rotational band contour of the origin band (measured at a temperature of  $\sim 55^\circ\text{C}$ ), they obtained  $\theta = \pm 42^\circ$ . This value is much lower than our value,  $\theta = \pm 62.2^\circ$ , and the question arises why the values are so different. The main reason is that Cané *et al.* did not take the axis reorientation effect into account. The hybrid character of their spectrum was determined by comparing the intensities of two sharp, unstructured features.<sup>21</sup> One of those features can be attributed to the  $'R$  branches ( $\Delta J = +1$ ,  $\Delta K_a = +1$ ) of the  $b$ -type band. The other feature contains both  $a$ -type and  $b$ -type transitions. We have simulated both features twice with two different sets of  $\theta$  and  $\theta_T$  values, namely,  $\theta = 42^\circ$  with  $\theta_T = 0^\circ$ , and  $\theta = 62.2^\circ$  with  $\theta_T = 1.0^\circ$ . Both simulations give approximately the same intensity ratios for the two features. Apparently, neglecting axis reorientation underestimates the value of  $\theta$ .

The same group analyzed the rotational band contour of benzimidazole.<sup>26</sup> For the direction of the transition moment, a value for  $\theta$  of  $\pm 18^\circ$  was found. Although axis reorientation was not taken into account, this value is remarkable close to the value of present study,  $\pm 22.0^\circ$ . Comparison of the band contours of benzimidazole<sup>26</sup> and indazole<sup>21</sup> shows that the "pure  $b$ -type feature" in benzimidazole is less pronounced than in the indazole contour. Therefore, Cané *et al.* have determined the hybrid character of benzimidazole by examining the shape of the *total* band contour. This method gives more or less the same result as an analysis with axis reorientation (compare the results of models 2 and 4 in Table II).

The rotational constants, given in Table I, are directly related to the geometrical structures in the ground state and the electronically excited state. All three molecules have a highly constrained geometry. Therefore, our data give no surprising conclusions. The molecules are mainly planar, in both states, since their inertial defects are small (i.e., close to zero). The equilibrium structure of a molecule is exactly planar, if its inertial defect is exactly zero. However, zero-point vibrational motion contributes to the inertial defect as well, leading to a small negative value of the inertial defect, even if the equilibrium geometry of the molecule is exactly planar.

Upon electronic excitation to the  $^1L_b$  state, the geometrical changes are similar in each molecule. The changes are small, and indicate a slight expansion of each molecule. These small geometrical changes are consistent with the results of vibrational spectroscopy. The fluorescence excitation spectra show intense  $0_0^0$  transitions and short Franck–Condon progressions. Only the "ring breathing" modes ( $760\text{ cm}^{-1}$  for the  $S_0$  state of indole<sup>9</sup>) form somewhat longer progressions (up to  $v=3$ ) in the excitation and fluorescence spectra of indole<sup>54</sup> and benzimidazole,<sup>23</sup> showing that the structural changes are mainly along these modes.

The rotational constants of indazole indicate that the transition at  $34\,472\text{ cm}^{-1}$  takes place in the 1H-tautomer. The ground state constants are identical to the constants found by Velino *et al.*,<sup>20</sup> who confirmed the 1H position via isotopic substitution. Since the differences between the rota-

TABLE IV. Experimental and calculated rotational constants and axis reorientation angles ( $\theta_T$ ) of indole. Calculated constants have been obtained from *ab initio* geometries (Refs. 53, 56). See text for further details.

	Rotational constants of indole in MHz		
	Experiment	3-21G	MP2/6-31G* and 3-21G
$A''$	3877.8	3950.0	3871.4
$B''$	1636.0	1648.3	1636.2
$C''$	1150.9	1163.0	1150.1
$\Delta A$	-134.8	-142.3	-138.7
$\Delta B$	-17.9	-13.8	-13.6
$\Delta C$	-20.7	-19.4	-19.1
$\theta_T$	$+0.5^\circ$	$+0.62^\circ$	$+0.62^\circ$

tional constants of the excited state and the ground state are similar to the differences in constants of indole and benzimidazole, we conclude that the indazole in the excited state is in the same form as in the ground state. These results are in agreement with those of Catalán *et al.*,<sup>27</sup> who concluded from spectroscopic and thermodynamical data that indazole exists as the 1H-tautomer, both in the ground and excited state.

New information about structural changes upon electronic excitation, is provided by the axis reorientation effect.<sup>55</sup> Rotational constants, obtained from a frequency analysis of the rotational resolved fluorescence excitation spectrum, contain information about the geometry in both states. The ground state rotational constants can provide structural information with respect to the principal axis system in the ground state, while the excited state constants can provide the excited state structure with respect to the principal axis system of the excited state. However, there is no information in the rotational constants about how both principal axis systems are oriented with respect to each other. This information, the axis reorientation angle(s), can be obtained from the intensities of the rotational lines. The axis reorientation angles of indole, indazole, and benzimidazole are small; respectively,  $\pm 0.50^\circ$ ,  $\pm 1.0^\circ$ , and  $\pm 0.7^\circ$  (however, the effect on the intensities, and therefore on the determination of the direction of the transition moment, is quite large).

The sign of the axis reorientation angle  $\theta_T$  is related directly to the sign of the angle between the transition moment vector and the  $a$ -axis,  $\theta$  (see Table I). Therefore, if the direction of the transition moment is known, for example by comparing  $\theta$  of substituted and unsubstituted molecules, this will give immediately the sign of  $\theta_T$  (and vice versa). For indole the sign of  $\theta$  is positive, and therefore  $\theta_T$  is positive;  $+0.5^\circ$ . Since the axis reorientation angles of indole, indazole, and benzimidazole are rather small, it is difficult to determine which atomic displacements are responsible for the rotation of the inertial axes.

The rotational constants in the ground and in the electronically excited states, and the axis reorientation angles presented in this chapter, can be used for testing *ab initio* calculations and for improving semiempirical calculations of both electronic states. As an example, the experimental constants of indole are compared with the results from *ab initio* calculations of Slater and Callis.<sup>53</sup> Table IV shows the ex-

perimental (first column) and calculated rotational constants. The rotational constants in the second column, have been calculated from the geometries obtained by using the 3-21G basis set for the ground state and the  ${}^1L_b$  state (however, the excited state involves single configuration interaction). The ground state constants in the last column have been calculated from the optimized geometry from a MP2/6-31G\* calculation. This level gives the best agreement with the vibrational frequencies in the ground state (without scaling).<sup>53</sup> The excited state geometry, used to calculate the differences in the rotational constants (last column of Table IV), has been calculated using the MP2/6-31G\* ground state with the geometry differences from the 3-21G geometries. The same method has been used by Callis, Slater, and Vivian<sup>56</sup> to calculate the fluorescence spectrum from the  ${}^1L_b$  origin which is in good agreement with the experimental spectrum.

In order to calculate the axis reorientation angle from *ab initio* geometries for a planar molecule with in-plane axis reorientation, the ground and excited state atomic coordinates should be expressed in their inertial axis systems, respectively  $(a''_i, b''_i, c''_i)$  and  $(a'_i, b'_i, c'_i)$ , where the *c*-axes are coinciding and perpendicular to the plane of the molecule. The axis reorientation angle is then given by<sup>33</sup>

$$\tan \theta_T = \frac{\sum_i m_i (a'_i b''_i - b'_i a''_i)}{\sum_i m_i (a'_i a''_i + b'_i b''_i)}, \quad (13)$$

where  $m_i$  are the atomic masses. This formula takes automatically into account the Eckart conditions. Table IV shows that the calculated values of  $\theta_T$  are in good agreement with the experimental values.

## VI. SUMMARY

We have measured the rotationally resolved spectra of the origin bands of the  $S_1({}^1L_b) \leftarrow S_0$  transitions of indole, indazole, and benzimidazole. From a frequency analysis of these spectra, the rotational constants in the ground and electronically excited states, have been obtained. All three molecules are planar in both states. Upon electronic excitation the molecules expand slightly. The intensities of the rotational lines are "perturbed" due to an in-plane reorientation of the *a* and *b* inertial axes upon electronic excitation. The intensities of the rotational lines are determined by the ground state population distribution ("the rotational temperature"), the hybrid band character, and the axis reorientation effect. The hybrid band character is related to the direction of the electronic transition moment vector with respect to the inertial axes. The intensity shapes of the spectra have been fit using various models (Table III). The best results have been obtained using a three parameter two-temperature rotational state distribution (non-Boltzmann), effects of inertial axes reorientation, and a Voigt line profile for each rotational transition. The axis reorientation angle  $\theta_T$  provides information about structural changes upon electronic excitation, which is additional to that obtained from the changes in the rotational constants. The data presented in this study, can be compared with results from *ab initio* and semiempirical calculations for the ground state and the excited state ( ${}^1L_b$  state). In this way,

these calculations can be improved to predict the properties of the second excited state, the  ${}^1L_a$  state, more precisely.

## ACKNOWLEDGMENTS

We would like to thank Professor P. R. Callis for providing us the *ab initio* geometries of indole prior to publication. Erko Jalviste gratefully acknowledges the support of the Nederlandse Organisatie voor Wetenschappelijk Onderzoek (NWO) and the Estonian Science Foundation (Grant No. 364). This work was made possible by financial support from the Dutch Foundation for Fundamental Research on Matter (FOM).

- <sup>1</sup>H.-U. Schütt and H. Zimmermann, Ber. Bunsenges. Phys. Chem. **67**, 54 (1963).
- <sup>2</sup>J. R. Platt, J. Chem. Phys. **19**, 101 (1951).
- <sup>3</sup>Y. Nibu, H. Abe, N. Mikami, and M. Ito, J. Phys. Chem. **87**, 3898 (1983).
- <sup>4</sup>J. W. Hager and S. C. Wallace, J. Phys. Chem. **87**, 2121 (1983).
- <sup>5</sup>R. Bersohn, U. Even, and J. Jortner, J. Chem. Phys. **80**, 1050 (1984).
- <sup>6</sup>See, for example, H. Lami and N. Glasser, J. Chem. Phys. **84**, 597 (1986).
- <sup>7</sup>See, for example, A. A. Rehms and P. R. Callis, Chem. Phys. Lett. **140**, 83 (1987).
- <sup>8</sup>B. J. Fender, D. M. Sammeth, and P. R. Callis, Chem. Phys. Lett. **239**, 31 (1995).
- <sup>9</sup>T. L. O. Barstis, L. I. Grace, T. M. Dunn, and D. M. Lubman, J. Phys. Chem. **97**, 5820 (1993).
- <sup>10</sup>S. Arnold and M. Sulkes, J. Phys. Chem. **96**, 4768 (1992), and references therein.
- <sup>11</sup>M. J. Tubergen and D. H. Levy, J. Phys. Chem. **95**, 2175 (1991).
- <sup>12</sup>P. L. Muiño and P. R. Callis, Chem. Phys. Lett. **222**, 156 (1994).
- <sup>13</sup>M. R. Eftink, L. A. Selvidge, P. R. Callis, and A. A. Rehms, J. Phys. Chem. **94**, 3469 (1990).
- <sup>14</sup>A. Mani and J. R. Lombardi, J. Mol. Spectrosc. **31**, 308 (1969).
- <sup>15</sup>L. A. Philips and D. H. Levy, J. Chem. Phys. **85**, 1327 (1986).
- <sup>16</sup>R. D. Suenram, F. J. Lovas, and G. T. Fraser, J. Mol. Spectrosc. **127**, 472 (1988).
- <sup>17</sup>W. Caminati and S. di Bernardo, J. Mol. Struct. **240**, 253 (1990).
- <sup>18</sup>E. Cané, P. Palmieri, R. Tarroni, and A. Trombetti, J. Chem. Soc. Faraday Trans. **89**, 4005 (1993).
- <sup>19</sup>J. P. Byrne and I. G. Ross, Aust. J. Chem. **24**, 1107 (1971).
- <sup>20</sup>B. Velino, E. Cané, and A. Trombetti, J. Mol. Spectrosc. **155**, 1 (1992).
- <sup>21</sup>E. Cané, A. Trombetti, B. Velino, and W. Caminati, J. Mol. Spectrosc. **155**, 307 (1992).
- <sup>22</sup>R. D. Gordon and R. F. Yang, Can. J. Chem. **48**, 1722 (1970).
- <sup>23</sup>E. Jalviste and A. Treshchalov, Chem. Phys. **172**, 325 (1993).
- <sup>24</sup>The absolute frequencies of the  $0_0^0$  bands reported in Ref. 23 have been calibrated with neon emission lines. Unfortunately, their wavelengths have not been corrected to the vacuum. The corrected frequencies of the origins are  $34\,917\text{ cm}^{-1}$  for benzotriazole and  $36\,022\text{ cm}^{-1}$  for benzimidazole.
- <sup>25</sup>B. Velino, A. Trombetti, and E. Cané, J. Mol. Spectrosc. **152**, 434 (1992).
- <sup>26</sup>E. Cané, A. Trombetti, B. Velino, and W. Caminati, J. Mol. Spectrosc. **150**, 222 (1991).
- <sup>27</sup>J. Catalán, J. C. del Valle, R. M. Claramunt, G. Boyer, J. Laynez, J. Gómez, P. Jiménez, F. Tomás, and J. Elguero, J. Phys. Chem. **98**, 10 606 (1994).
- <sup>28</sup>G. Berden, E. Jalviste, and W. L. Meerts, Chem. Phys. Lett. **226**, 305 (1994).
- <sup>29</sup>B. Velino, E. Cané, L. Gagliardi, A. Trombetti, and W. Caminati, J. Mol. Spectrosc. **161**, 136 (1993).
- <sup>30</sup>W. Caminati (private communication).
- <sup>31</sup>F. Tomas, J. Catalán, P. Pérez, and J. Elguero, J. Org. Chem. **59**, 2799 (1994).
- <sup>32</sup>J. Catalán, P. Pérez, and J. Elguero, J. Org. Chem. **58**, 5276 (1993).
- <sup>33</sup>J. T. Hougden and J. K. G. Watson, Can. J. Phys. **43**, 298 (1965).
- <sup>34</sup>T. R. Huet, M. Godefroid, and M. Herman, J. Mol. Spectrosc. **144**, 32 (1990).
- <sup>35</sup>D. M. Jonas, X. Yang, and A. M. Wodtke, J. Chem. Phys. **97**, 2284 (1992).
- <sup>36</sup>R. E. Smalley, L. Wharton, D. H. Levy, and D. W. Chandler, J. Mol. Spectrosc. **66**, 375 (1977).

- <sup>37</sup>J. A. Konings, W. A. Majewski, Y. Matsumoto, D. W. Pratt, and W. L. Meerts, *J. Chem. Phys.* **89**, 1813 (1988).
- <sup>38</sup>A. Held, B. B. Champagne, and D. W. Pratt, *J. Chem. Phys.* **95**, 8732 (1991).
- <sup>39</sup>I. Özkan, *J. Mol. Spectrosc.* **139**, 147 (1990).
- <sup>40</sup>A. R. Chigirev, *Opt. Spectrosc.* **67**, 175 (1989); A. R. Chigirev, *Opt. Spectrosc.* **69**, 192 (1990).
- <sup>41</sup>W. Gordy and R. L. Cook, *Microwave Molecular Spectra*, 3rd ed. (Wiley, New York, 1984).
- <sup>42</sup>A Hamiltonian which is invariant under all operations of the Four group, can be factorized in four blocks by using the Wang functions as basis set. The Hamiltonian of Eq. (8) is invariant under the operations of the cyclic  $C_2(c)$  group. Use of the Wang functions as basis set, will factorize the Hamiltonian in two blocks. Therefore, the calculations are still being simplified by using this basis set.
- <sup>43</sup>D. F. Plusquellic and D. W. Pratt, *J. Chem. Phys.* **97**, 8970 (1992).
- <sup>44</sup>S. Gerstenkorn and P. Luc, *Atlas du Spectroscopie D'absorption de la Molecule D'iode* (CNRS, Paris, 1978); S. Gerstenkorn and P. Luc, *Rev. Phys. Appl.* **14**, 791 (1979).
- <sup>45</sup>G. Berden, Ph.D. thesis, University of Nijmegen, 1995.
- <sup>46</sup>S. Stolte, in *Atomic and Molecular Beam Methods*, edited by G. Scoles (Oxford University, New York, 1988), Vol. 1.
- <sup>47</sup>Y. R. Wu and D. H. Levy, *J. Chem. Phys.* **91**, 5278 (1989).
- <sup>48</sup>E. Pebay Peyroula and R. Jost, *J. Mol. Spectrosc.* **121**, 167 (1987).
- <sup>49</sup>J. M. Price, J. A. Mack, G. v. Helden, X. Yang, and A. M. Wodtke, *J. Phys. Chem.* **98**, 1791 (1994).
- <sup>50</sup>G. L. Blackman, R. D. Brown, F. R. Burden, and A. Mishra, *J. Mol. Struct.* **9**, 465 (1971).
- <sup>51</sup>L. A. Philips and D. H. Levy, *J. Phys. Chem.* **90**, 4921 (1986).
- <sup>52</sup>P. R. Callis, *J. Chem. Phys.* **95**, 4230 (1991).
- <sup>53</sup>L. S. Slater and P. R. Callis, *J. Phys. Chem.* **99**, 8572 (1995).
- <sup>54</sup>G. A. Bickel, D. R. Demmer, E. A. Outhouse, and S. C. Wallace, *J. Chem. Phys.* **91**, 6013 (1989).
- <sup>55</sup>However, if the ground *and* the excited state geometries of a molecule are known from isotopic substitution studies, the axis reorientation angle can be calculated from these geometries. In spite of this, the complete substitution structure in the excited state of a molecule as large as indole has not been determined yet.
- <sup>56</sup>P. R. Callis, J. T. Vivian, and L. S. Slater, *Chem. Phys. Lett.* **244**, 53 (1995).